Retinal Microvasculature Alteration in High Myopia

Ye Yang,[1,2] Jianhua Wang,[2] Hong Jiang,[2] Xiaoling Yang,[1] Limiao Feng,[1] Liang Hu,[1,2] Liang Wang,[3] Fan Lu,[1] and Meixiao Shen[1]

[1]School of Ophthalmology and Optometry, Wenzhou Medical University, Wenzhou, Zhejiang, China
[2]Department of Ophthalmology, Bascom Palmer Eye Institute, University of Miami, Miami, Florida, United States
[3]Krieger School of Arts and Sciences, Johns Hopkins University, Baltimore, Massachusetts, United States

Correspondence: Fan Lu, School of Ophthalmology and Optometry, Wenzhou Medical University, 270 Xueyuan Road, Wenzhou, Zhejiang 325027, China; lufan62@mail.eye.ac.cn.
Meixiao Shen, School of Ophthalmology and Optometry, Wenzhou Medical University, 270 Xueyuan Road, Wenzhou, Zhejiang 325027, China; shenmxiao7@hotmail.com.

Submitted: March 10, 2016
Accepted: October 10, 2016

Citation: Yang Y, Wang J, Jiang H, et al. Retinal microvasculature alteration in high myopia. *Invest Ophthalmol Vis Sci*. 2016;57:6020–6030. DOI: 10.1167/iovs.16-19542

Purpose. To investigate the retinal vascular network alterations in highly myopic eyes.

Methods. Thirty-three highly myopic eyes from 21 subjects and 47 mildly myopic or emmetropic eyes from 24 healthy control subjects were enrolled. Optical coherence tomography angiography (OCTA) was used to image the superficial, deep, and whole retinal vascular plexuses at the macular region. Highly myopic eye images were analyzed after adjusting the ocular magnification using Bennett's formula. Fractal analysis (box counting method, D_{box}) representing vessel density was performed in different annular and quadrantile zones of both large vessels and microvessels. Correlations between the vascular density, axial length, and spherical equivalent refractive error were analyzed.

Results. The average density (D_{box}) of the superficial retinal annular zone (0.6–2.5 mm) microvessels was 1.741 ± 0.018 in highly myopic eyes and was shown to be significantly lower than that of the controls (1.773 ± 0.010, $P < 0.001$). Individual annular zone (bandwidth of 0.16 mm) analysis of highly myopic eyes revealed a significant level of microvessel alteration in all zones compared with the same zones in control eyes ($P < 0.001$). Furthermore, in the highly myopic group, the microvessel density was significantly correlated with axial length elongation in all three layers ($r = -0.38$ to -0.48; $P < 0.05$).

Conclusions. This study reveals retinal microvascular network alterations in highly myopic eyes, which correlates with axial length elongation. Fractal analysis of the microvasculature by OCTA images may help to characterize the underlying pathophysiological mechanisms involved in high myopia.

Keywords: microvasculature, optical coherence tomography angiography, fractal analysis, high myopia

The prevalence of high myopia has been increasing worldwide, particularly in East Asia.[1,2] Along with the increase in refractive error and axial length, highly myopic eyes frequently suffer from fundus vascular lesions such as macular hemorrhage and choroid neovascularization.[3,4] Previous studies have focused on the relationship between high myopia and large retinal vascular changes. Using color Doppler imaging, Benavente-Perez et al.[5] demonstrated a pulse amplitude reduction in the central retinal artery of highly myopic eyes. With a fundus camera and fractal analysis, Azemin et al.[6] analyzed the retinal vessels in moderate to high myopia and found a density reduction in the large retinal vessels of myopic eyes when compared with emmetropic eyes. While large retinal vessel impairment is evident in myopic eyes, analyzing the impact of myopia on retinal microvessels has remained elusive, mainly due to technical difficulties.

The recent development of optical coherence tomography angiography (OCTA) enables noninvasive imaging and analysis of both large retinal vessels and microvessels.[7,8] Moreover, this technique provides detailed information, allowing visualization of the retinal vessel network in multiple layers.[9] The characterization of microvascular alterations in the retina may broaden our understanding of visual compromise in highly myopic eyes. To quantitatively study microvascular network alterations in the retina, we developed an analytical algorithm to segment the retinal vascular network for fractal analysis.[10] The aim of this study was to investigate the retinal microvascular network alterations in myopic eyes through quantitative retinal microvessel density analyses using OCTA.

Materials and Methods

Patients from the Wenzhou Eye Hospital (Wenzhou, China) and students from Wenzhou Medical University (Wenzhou, China) were recruited. This cross-sectional study was approved by the Ethics Committee of Wenzhou Medical University and performed in accordance with the Declaration of Helsinki principles. A consent form was signed by each subject. The enrolled subjects were divided into two groups according to their spherical equivalents (SEs). Emmetropic and mildly myopic subjects with SEs ranging from +0.50 to −3.00 diopters (D) were designated as the control group. Subjects with SEs less than −6.00 D were designated as the highly myopic group. Each subject underwent a complete ocular examination including best-corrected visual acuity (BCVA), intraocular pressure (IOP) by Goldmann applanation tonometry, slit-lamp examination, funduscopy, visual field testing, and axial length (AL) measurement by optical biometry (IOL Master; Carl Zeiss Meditec, Jena, Germany). The inclusion criteria for both groups were as

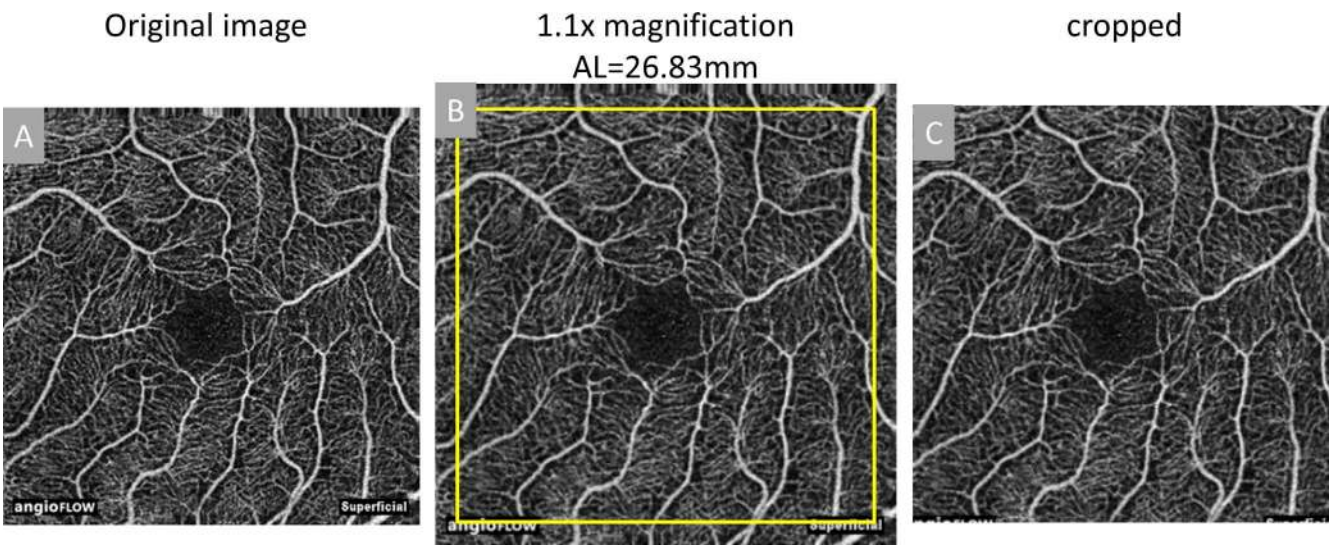

FIGURE 1. Magnification correction of high myopia images. The original image (**A**) was magnified 1.1× according to the axial length (AL = 26.83 mm) to create the magnified image (**B**), which was further cropped to the size of the original image (**C**).

follows: 18 to 40 years old, BCVA equal to or better than 20/20, refractive error $< +0.5$ D, astigmatism < -1.00 D, and a refractive error with less than 2.00-D difference between the two eyes. The exclusion criteria were myopic macular degeneration, any history of vitreoretinal disease, IOP > 21 mm Hg, visual field defects, history of intraocular surgery or systemic diseases potentially affecting the eyes.

After ocular examination, all subjects were imaged by a single operator (XY) using an RTVue XR Avanti Spectral Domain OCT system (Optovue, Inc., Fremont, CA, USA) equipped with AngioVue software (Version 2015.1.0.90). The eye movement was offset during image processing using the Motion Correction Technology (MCT) function to correct the horizontal and vertical scans.[11] The scan speed was set to 70,000 A-scans per second. One OCTA scan included both an X-scan and a Y-scan, and lasted approximately 2.9 seconds for each of the two raster scans.[12] The total scan time was approximately 6 seconds. The scan area was centered on the fovea with a field of view of 3×3 mm^2, which corresponded to approximately 10°. The resolution of the exported OCT images was 304 × 304 pixels. A good set of scans, with a signal strength index (SSI) of >40 for each eye, was selected for further analysis. Any image with either a doubled vessel pattern or other motion artifacts extending over more than three lines was excluded. Optical coherence tomography angiography images of the superficial, deep, and whole retinal layers were used after segmentation. The Split-Spectrum Amplitude-Decorrelation Angiography (SSADA) algorithm was used to segment the vessels.[13] The superficial layer was segmented from 3 μm beneath the inner limiting membrane (ILM) to 15 μm beneath the inner plexiform layer (IPL), representing the outer boundary of the ILM to the outer boundary of the IPL. The deep layer was segmented from 15 μm beneath the IPL to 70 μm beneath the IPL, representing the outer boundary of the IPL to the outer boundary of the outer plexiform layer (OPL).[8,14] The whole retinal layer was segmented from 3 μm beneath the ILM to 30 μm beneath the retinal pigment epithelium (RPE) layer, according to the manufacturer's instructions. The superficial retinal layer is composed of the ganglion cell and inner plexiform layers, whereas the deep retinal layer is composed of the inner nuclear and outer plexiform layers. These layers encompass the entire retinal vascular network.[15]

Because the magnification is different in myopic eyes, the imaging sampling density in myopic eyes must be lower than in normal eyes. Therefore, images obtained from highly myopic eyes were corrected for magnification using Bennett's formula.[16,17] The relationship between OCT image measurements and actual scan diameter was expressed by the formula $t = p \times q \times s$, where t represents the actual scan length, p represents the magnification factor determined by the OCT imaging system camera, q represents the magnification factor in relation to the eye, and s represents the original measurement value obtained from the OCT image. The correction factor q is expressed by the equation $q = 0.01306 \times (AL - 1.82)$ (Fig. 1).

In highly myopic eyes, due to axial elongation and longer focal length, the lateral resolution of the retina is potentially diminished. When raw images are used for quantification, the lateral resolution may adversely affect the density calculation. A previously described image segmentation and skeletonized analysis algorithm was used to quantitatively study the macular microvascular network.[10] Briefly, the Matlab (The Mathworks, Inc., Natick, MA, USA) custom algorithm automatically segments the vascular network (i.e., large vessels and microvessels) using a series of processing procedures, including image inversion equalization, background noise correction, and nonvessel structure removal (Fig. 2). Our custom algorithm separates the vessels with diameters > 25 μm in both the superficial and deep layers. The large vessels in the superficial vascular plexus were used for further analysis. The large vessels in the deep layer have been suggested to be graphic projection shadow artifacts (Fig. 3).[18] The removal of the large vessel projection from the deep layer may reduce these artifacts when the fractal dimension of the microvascular network in the deep layer is analyzed. Therefore, large vessels were defined by a width ≥ 25 μm and microvessels by a width < 25 μm. The segmented vessel image was then converted into a binary image and skeletonized for fractal analysis. The skeletonized images were divided into six annular zones (C1–C6, centered on the fovea) after removal of the avascular zone (diameter = 0.6 mm). The bandwidth of each annular zone was 0.16 mm. In addition to these thin individual annular zones, the total annular zone (bandwidth of 1.9 mm) was also analyzed. Furthermore, the total annular zone was divided into quadrantal angles (90°) defined as the superior nasal, superior temporal, inferior nasal, and inferior temporal sectors (Fig. 2).

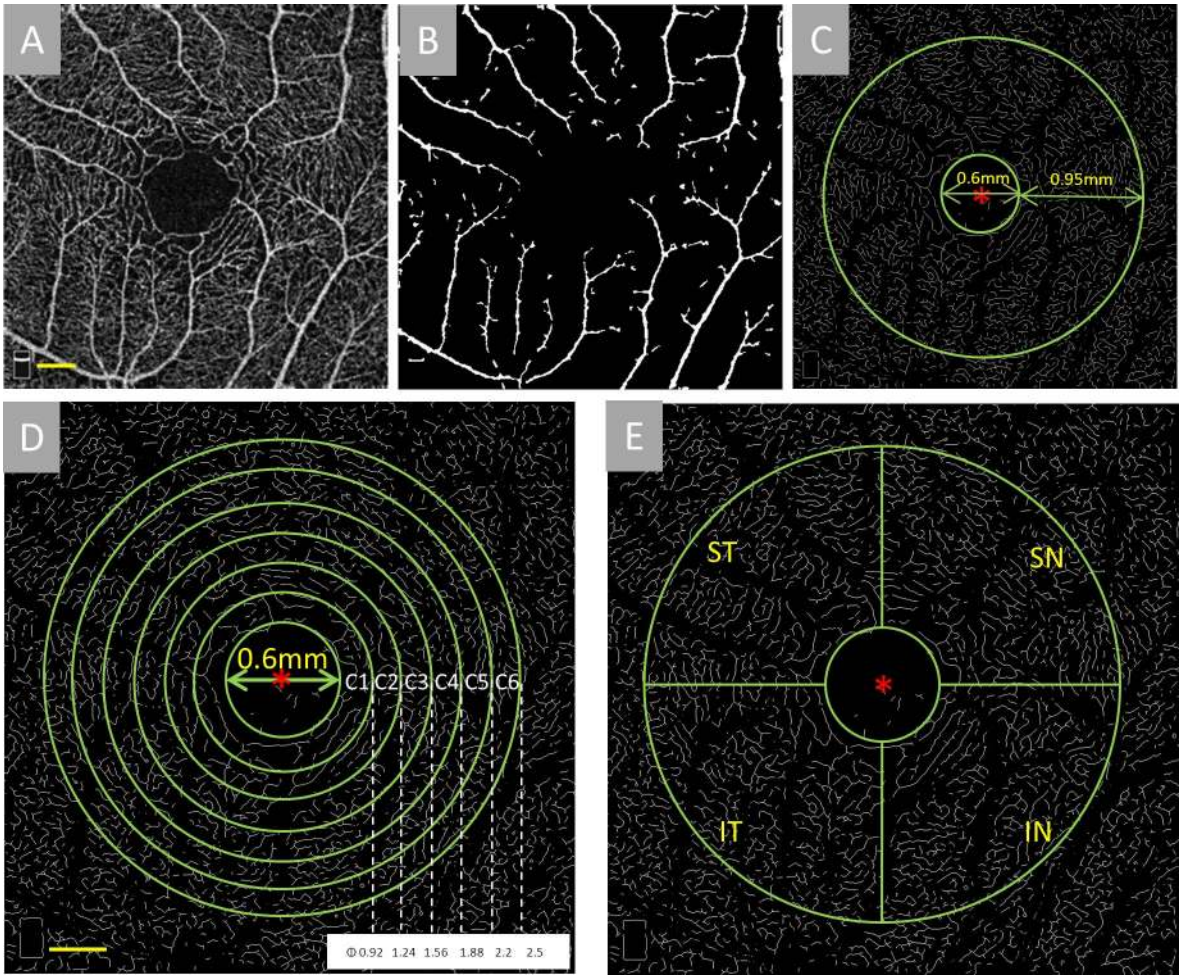

FIGURE 2. Image processing and partitioning method. The raw image (**A**) was acquired using OCTA, centered on the fovea, with a field of view of 3 × 3 mm^2. Large retinal vessels, with a diameter >∼25 μm, were segmented and extracted (**B**). The remaining microvessels on microvascular network images were then skeletonized (**C**), and the annular zone (0.6–2.5 mm) was used for analysis after the removal of the avascular zone (diameter = 0.6 mm). The annular zone (0.6–2.5 mm) was divided into six annuli (C1–C6, centered on the fovea), with a bandwidth of 0.16 mm (**D**). In addition, four quadrant zones were generated and centered on the fovea (**E**). ST, superior temporal; SN, superior nasal; IT, inferior temporal; IN, inferior nasal. *Scale bar*: 300 μm.

In addition, to examine the effect on microvessel density estimates resulting from the use of an arbitrary vessel width cutoff (i.e. 25 um), vessel density was also processed using the same method as described above, without removal of the large vessels.

Fractal analysis is commonly used to investigate the vascular network in fundus images[6,19,20] or to quantitatively analyze large retinal vessel density in myopic eyes.[6,19] In the present study, the fractal analysis toolbox from Benoit (TruSoft Benoit fractal analysis toolbox; TruSoft International, Inc., St. Petersburg, FL, USA) was incorporated into our custom algorithm to analyze the fractal dimensions (representing vessel density) of the large retinal vessels and microvessels on the segmented vascular network images. The fractal dimension (D_{box}) was measured using the box-counting technique. The pixel size of the largest box for counting nonempty boxes was set to 104 pixels, and the incremental rotation degree of the grid in searching nonempty boxes was set to 15°, which was in accordance with the default software settings. Analysis repeatability was assessed in 10 control and 10 myopic eyes. The combination of annuli C1 to C6 minus the avascular zone ("combined annuli") was also analyzed.

The refraction data were converted to SEs (SE = spherical dioptric power plus one-half of the cylindrical dioptric power). The repeated measurement analysis of variance (Re-ANOVA) was used for overall effects. Post hoc paired *t*-tests with Fisher correction were used to determine the existence of pairwise differences between different zones and groups. Independent sample *t*-tests were used to assess biographic differences between the groups. Correlations between macular vessel density and AL were determined using the Pearson's correlation test. A receiver operating characteristic (ROC) curve was also calculated to confirm the feasibility of determining vascular network alterations in highly myopic eyes from OCTA vessel analyses. All data were expressed as the mean ± standard deviations and were analyzed using SPSS software (version 19.0; SPSS, Inc., Chicago, IL, USA). $P < 0.05$ was considered to be significantly different.

RESULTS

Demographics of the enrolled subjects are shown in Table 1. There was no significant difference in age or sex ($P > 0.05$) between the high myopia ($n = 21$) and control groups ($n = 24$).

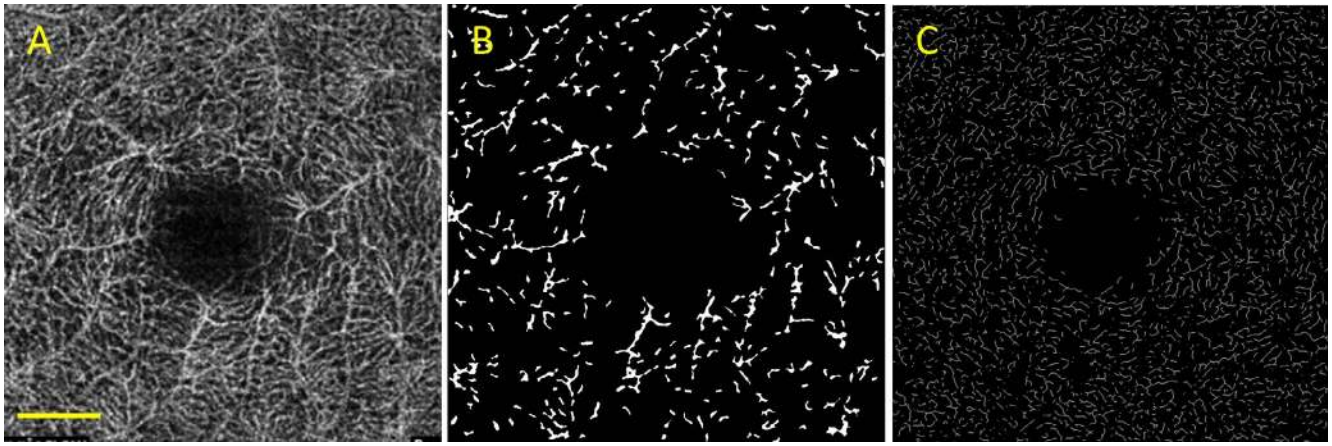

FIGURE 3. Removal of shadowgraphic projection artifacts in the deep vascular network. (**A**) The raw OCTA image of deep retinal vascular plexus. (**B**) Large vessel segmented from the raw image of deep retinal vascular plexus. (**C**) Microvasculature skeletonized after the large vessel was extracted from the deep retinal vascular plexus. *Scale bar*: 500 μm.

The ALs and SEs were significantly different between the two groups ($P < 0.05$).

The microvessels and large vessels were clearly visualized in all vascular network maps (Fig. 4). In the superficial layer, the large vessels and microvessels in the high myopia group were significantly lower in density when compared with controls. In the deep retinal layer, the two groups had similar large vessel densities, but microvessels were significantly less dense in highly myopic eyes. The whole retinal layer was similar to the superficial layer in that the large retinal vessel and microvessel densities were both significantly lower in highly myopic eyes when compared to the controls (Table 2; Fig. 5). The coefficients of repeatability and reproducibility (C_OR) for the D_{box} values of microvessels were 0.04 (2.4%), 0.03 (1.8%), and 0.03 (1.6%) in the superficial, deep, and whole retinal layers, respectively. For large vessels, the C_OR of the D_{box} values was 0.05 (4.8%), 0.04 (3.4%), and 0.04 (3.8%) in the superficial, deep, and whole retinal layers, respectively.

The total annular zone was divided into four quadrantal zones and six annular zones (bandwidth = 0.16 mm). With the exception of the superior temporal quadrant in the deep retinal layer ($P = 0.06$), the microvessel density within the total annular zone was significantly lower in the highly myopic group than in the control group for all quadrantal zones of the superficial, deep, and whole retinal layers (Fig. 6, all $P < 0.05$). The large vessel density in the high myopia group was significantly lower in the superior nasal and inferior nasal zones when compared with the controls (Fig. 6, all $P < 0.05$). The microvessel densities in all individual annular zones (C1–C6) of the superficial, deep, and whole retinal layers were significantly lower in highly myopic subjects than in controls (Fig. 7, all $P < 0.05$).

The microvessel densities in the superficial ($r = -0.38$; $P = 0.02$), deep ($r = -0.35$; $P = 0.045$), and whole ($r = -0.48$; $P = 0.004$) retinal layers correlated with AL elongation (Fig. 8). The large vessels in the superficial ($r = -0.59$; $P = 0.002$) and whole ($r = -0.39$; $P = 0.02$) retinal layers correlated with AL elongation. Only the whole retinal layer microvessel densities ($r = 0.40$; $P = 0.02$) correlated with SE. The large vessel densities in the superficial ($r = 0.12$; $P > 0.05$), deep ($r = 0.15$; $P > 0.05$), and whole ($r = 0.12$; $P > 0.05$) retinal layers did not significantly correlate with the SE.

In the ROC curve analysis (Fig. 9), the retinal microvessel density areas under the curve (AUC) were 0.96 ($P < 0.001$), 0.97 ($P < 0.001$), and 0.94 ($P < 0.001$) in the superficial, deep, and whole retinal layers, respectively, with total annular zone (0.6–2.5 mm) cutoff D_{box} values of 1.765, 1.765, and 1.775, respectively. These microvessel density analysis parameters provided sensitivities of 94%, 93%, and 85% for each layer, respectively, with specificities of 87%, 89%, and 96% for each layer, respectively, for the microvascular network impairment in highly myopic eyes. After combining the density results of the superficial and deep retinal microvessels, the AUC became 0.987 ($P < 0.001$) with a cutoff value of 3.12, which yielded sensitivity and specificity values of 100% and 95.7%, respectively. In the four quadrantal zones, the AUC values were 0.86 ($P < 0.001$), 0.87 ($P < 0.001$), and 0.89 ($P < 0.001$) for microvessel density (D_{box}) in the superficial inferior nasal, deep inferior nasal, and the whole retina inferior nasal quadrants. Likewise, the AUC for the C5 annular zone (1.88–2.20 mm) was 0.96 ($P < 0.001$), 0.98 ($P < 0.001$), and 0.96 ($P < 0.001$) in the three layers, respectively.

TABLE 1. Demographic Parameters of High Myopia and Control Groups

Parameters	Control*	High Myopia*	*P* Value
Number of eyes	47	33	-
Number of subjects	24	21	-
Age, y, range	27.4 ± 6.4	26.0 ± 2.7	0.36†
Sex, male/female	14/10	12/9	0.94†
SE, D, range	-0.77 ± 1.01 (0.50 to −2.50)	-8.68 ± 1.87 (−6.00 to −12.00)	<0.05†
AL, mm, range	23.84 ± 0.82 (22.01 to 25.06)	27.11 ± 1.27 (24.57 to 29.43)	<0.05†

* Mean ± SD.
† *t*-test.

DISCUSSION

In highly myopic eyes, the decline in retinal vascular network is viewed as an indicator of macular retinopathy progression, which commonly manifests as retinal vasculopathies.[14,21] Often, the onset of early macular retinopathy occurs without alterations of visual acuity. Previous studies reported conflicting results regarding retrobulbar and retinal large vessel alterations in myopic eyes (Table 3). Based on fundus images, a reduction in the large retinal vessel density was associated with myopia.[6,19] However, Chueng et al.[22] found no difference between myopic and normal eyes after correcting for field of

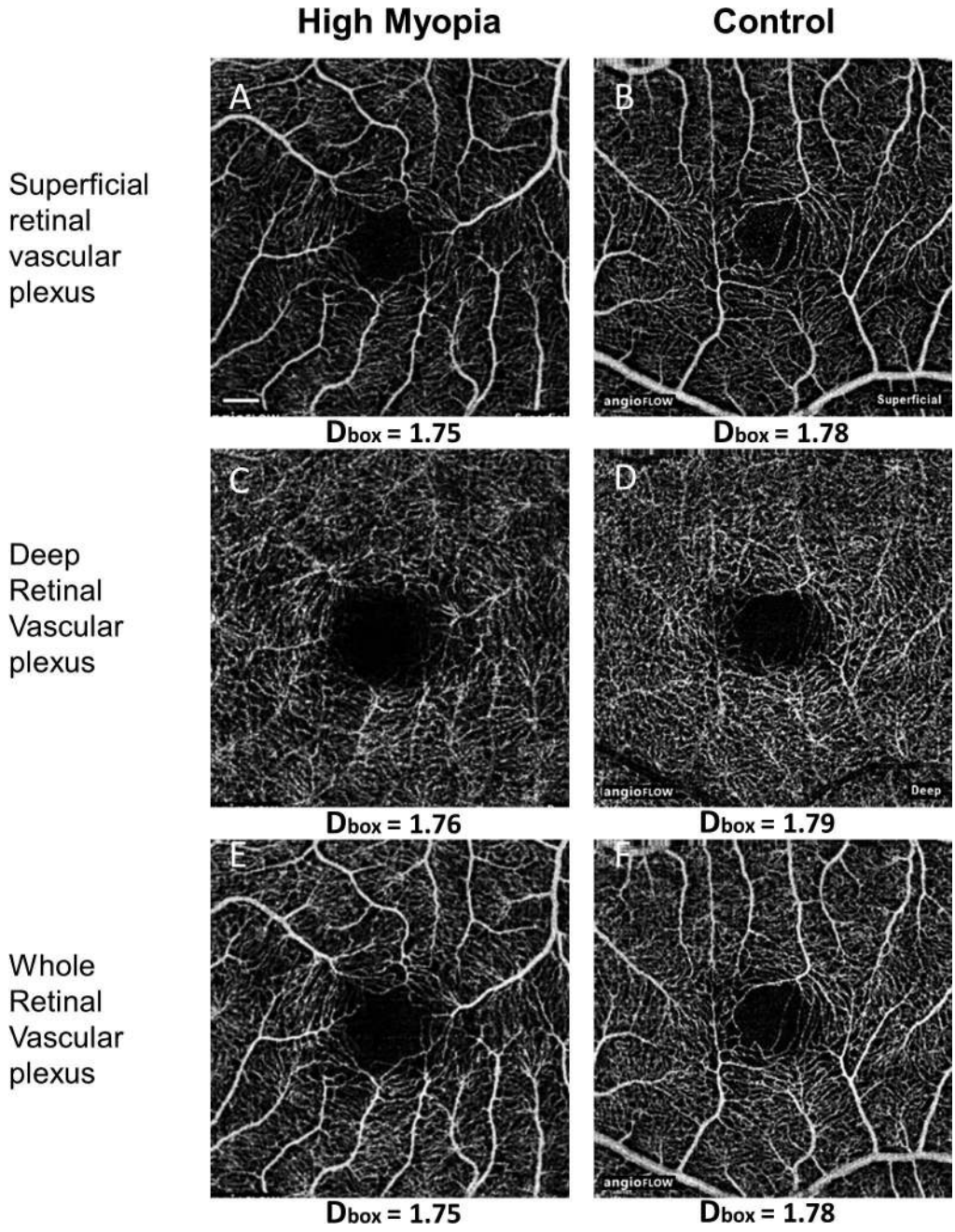

FIGURE 4. Representative OCTA images of highly myopic and control eyes. Superficial retinal vascular plexus in a highly myopic (**A**) and control eye (**B**). Deep retinal vascular plexus in a highly myopic (**C**) and control eye (**D**). Whole retinal vascular plexus in a highly myopic (**E**) and control eye (**F**). *Scale bar*: 300 μm.

view magnification. Hollo et al.,[23] using the Heidelberg retina flowmeter, reported that capillary perfusion near the temporal edge of the optic disc was significantly decreased in healthy subjects and glaucoma patients with myopia. However, the tests and analyses of large retinal vessels and global flow may not reflect the early onset of retinal vascular alterations before the manifestation of obvious vasculopathies. The retinal microvascular network, when imaged using noninvasive methods such as OCTA, may reveal alterations specific to myopic eyes and allow detection of preclinical retinopathy in myopic individuals.

Optical coherence tomography angiography enables noninvasive imaging of the retinal microvascular network, which allows for the in-depth analysis of retinal vessels that were previously invisible on fundus images.[29,30] In addition to the visualization of the overall retinal vascular network, OCTA provides the opportunity to acquire images and analyze the retinal vasculature in multiple layers, such as the superficial, deep, and whole retinal layers.[31] Similar to what is seen with traditional optical coherence tomography, AL impacts optical magnification, altering the actual scan size and potentially interfering with vessel caliber measurement.[22] Specifically, a longer AL will make the vascular network appear artificially denser because of the larger area being scanned under smaller magnification. The currently available OCTA systems do not provide a magnification correction feature, preventing direct

Table 2. Total Vessel Density (D_{box}) in the Different Retinal Layers of High Myopia and Control Groups (Mean ± SD) With and Without Large Vessels Separated

Vessel Patterns and Layers	High Myopia, $n = 21$	Control, $n = 24$	*P* Value
Large vessels separated			
Superficial microvessels	1.741 ± 0.018	1.773 ± 0.010	<0.001
Superficial large vessels	1.035 ± 0.023	1.061 ± 0.010	<0.001
Deep microvessels	1.746 ± 0.015	1.782 ± 0.010	<0.001
Deep large vessels	1.050 ± 0.017	1.052 ± 0.019	0.94
Whole retina microvessels	1.754 ± 0.015	1.784 ± 0.008	<0.001
Whole retina large vessels	1.048 ± 0.017	1.063 ± 0.010	0.001
Large vessels not separated			
Superficial	1.771 ± 0.031	1.803 ± 0.009	<0.001
Deep	1.775 ± 0.012	1.803 ± 0.008	<0.001
Whole retina	1.783 ± 0.014	1.809 ± 0.008	<0.001

comparison of results from highly myopic and normal individuals. In the present study, the decreased vessel density in highly myopic eyes became evident after magnification correction. Indeed, our results showed retinal microvascular network alterations across multiple retinal layers.

The Bennett formula includes a fixed value of 1.82 mm, which is the assumed distance from corneal vertex to the second principal plane. The second principal plane is defined as a refraction plane in the Gaussian schematic eye system,[16] through which any light parallel to the optical axis focuses on the retina. In the Bennett et al.[16] paper, variations of up to 2.26 mm were observed in highly myopic eyes. This would equate to an error of 1.85% in an eye with a 26-mm AL. To confirm the impact of the possible error due to a deep anterior chamber, we reprocessed the eyes with ALs of ~26 mm. We found four eyes with ALs of 26.26, 26.25, 26.38, and 26.32 mm, changed the fixed value from 1.82 to 2.26, and then calculated the magnification ratio. The magnification ratio produced a theoretical error of 1.85%. However, the differences in D_{box} in the 0.6- to 2.5-mm annuli were 0.1% (whole retina), 0.05% (superficial capillary plexus), and 0.29% (deep capillary plexus). Therefore, the possible error due to a deep anterior chamber does not adequately explain the differences in the fractal dimensions of the retinal microvasculature in the present study.

Our results are in agreement with previous studies using a fundus camera and other methods (e.g., fluorescein angiography and flowmetry).[6,19] Indeed, OCTA revealed alterations in both the superficial and deep retinal vascular plexuses, which indicates that alterations occur throughout the entire retina. Considering that the degree of decreased microvascular density correlated with axial elongation, the significantly altered microvascular network in highly myopic eyes may represent disease progression.

We also analyzed microvessel density in six annular zones and four quadrantal zones of the superficial, deep, and whole retinal layers. These densities were significantly lower in highly myopic subjects compared to controls, suggesting that the retinal microvasculature of highly myopic eyes is affected by diffuse alterations rather than isolated local changes. Decreased retinal thickness[32] and inner retinal layer dysfunction[33] have been linked to high myopia. A decline in microvessel density may be caused by reduced blood supply demands due to the retinal degeneration occurring in highly myopic eyes. Alternatively, the retinal dysfunction may be caused by compromise to the retinal vasculature, secondary to axial elongation, which would seem to unavoidably stretch the retinal vasculature. This is a chicken-and-egg question in terms of which comes first, which warrants further longitudinal studies. Retinal vessel caliber narrowing in highly myopic eyes may also contribute to reduced density,[20,27] as the decrease in retinal blood supply likely results in capillary network loss. Decreases in blood flow in highly myopic eyes have been reported for both retrobulbar and retinal microvasculature.[5,24,26] Furthermore, using ultra-wide fluorescein angiography, Hollo et al.[23] identified a larger nonperfused zone in the far retinal periphery of highly myopic eyes. This nonperfused area may be caused by retinal stretching, which may further exacerbate peripheral retina thinning. These structural changes may eventually cause retinal microvessel loss and induce retinal capillary regression.[23] The significant correlation between the microvessel density and AL may also suggest that the global elongation may affect the retinal microvasculature. The stretching of the sclera, choroid, and retina caused by AL elongation may result in retinal and choroidal thinning. Retinal atrophy and choroid thickness reduction may further decrease oxygen requirements and consequently decrease blood flow.[26] It is also possible that nonperfused zones in the retina appear because of the reduced retrobulbar blood flow associated with myopia, something not detectable by OCTA scanning. However, whether these structural alterations occur before or after the vascular alterations remains unclear. Additional longitudinal studies are required to determine the sequence of events surrounding these alterations.

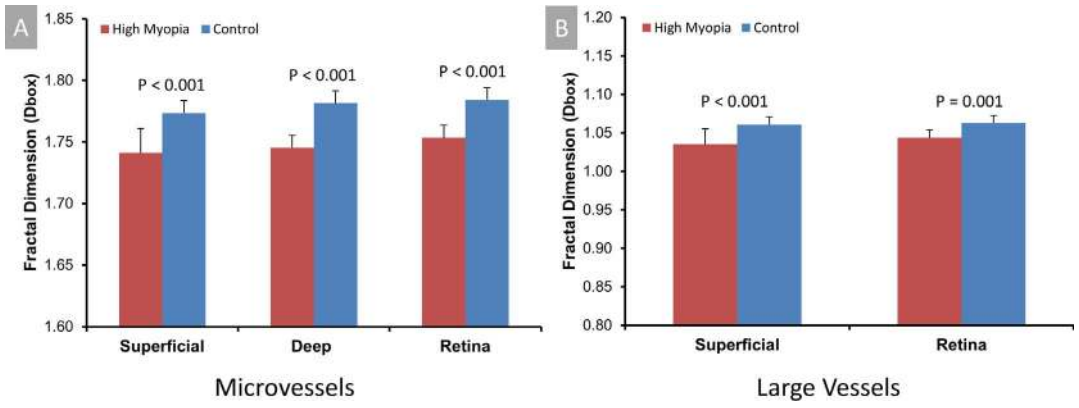

Figure 5. Vessel density (D_{box}) comparison between high myopia and control groups for microvessels and large vessels. (**A**) The microvessel density in the total annular zone (0.6–2.5 mm) of highly myopic eye was significantly lower than that in the control eyes for all retinal layers (superficial, deep, and whole) (all $P < 0.001$). (**B**) The large vessel densities in the total annular zone (0.6–2.5 mm) of the highly myopic eyes were significantly lower than in the control eyes for the superficial ($P < 0.001$) and whole ($P = 0.001$) retinal layers.

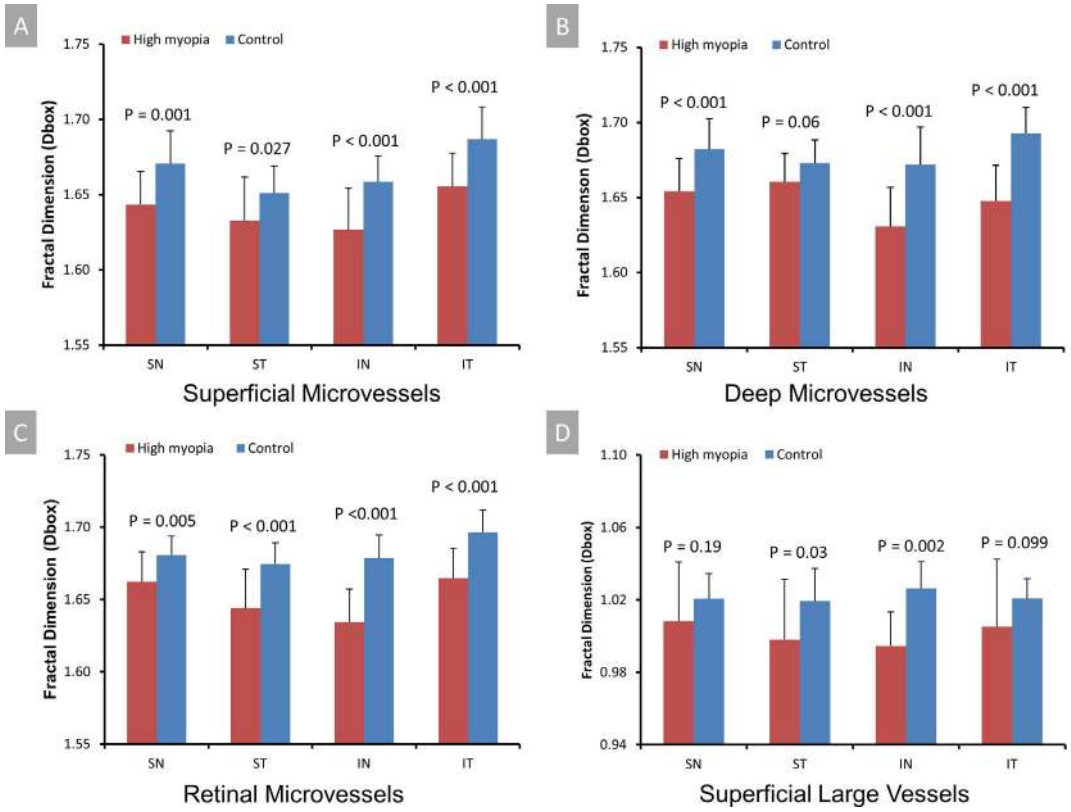

Figure 6. Quadrantal microvessel and large vessel density (D_{box}) comparisons between highly myopic and control subjects for each layer. In the high myopia group, except for the superior temporal sector of the deep retinal layer ($P = 0.06$), the microvessel density was significantly lower than in the control group for all quadrantal zones of the superficial (**A**), deep (**B**), and whole (**C**) retinal layers (all $P < 0.05$). The large vessel density in the high myopia group was significantly lower in the superior nasal and inferior nasal zones compared with those of the control group ([**D**] $P < 0.05$). SN, superior nasal; ST, superior temporal; IN, inferior nasal; IT, inferior temporal.

Receiver operating characteristic curve analysis may help determine the discriminating power of vasculature impairments in myopic eyes. In the present study, the areas under the ROC curve for annular zones were higher than those for quadrantal zones, indicating diffuse microvessel alterations in highly myopic eyes. The microvessel density changes held considerably more discriminating power for vascular impairment determination than for other measurements. Furthermore, the C5 annular zone (1.88–2.2 mm) had the highest AUC when compared with other zones, which may be a result of increased thinning in the parafoveal area versus the foveal area in highly myopic eyes.[32] As expected, the combined microvessel density of the superficial and deep retinal layers returned the highest AUC value. Therefore, this measurement could be used as an early macular retinopathy surrogate endpoint in clinical trials involving myopic patients.

We used fractal analysis to indicate the microvessel density in the macula, which is different from the study of Pinhas et al.,[34] in which vessel density was reported as a percentage. The magnitude of the changes in fractal dimensions (no unit) may

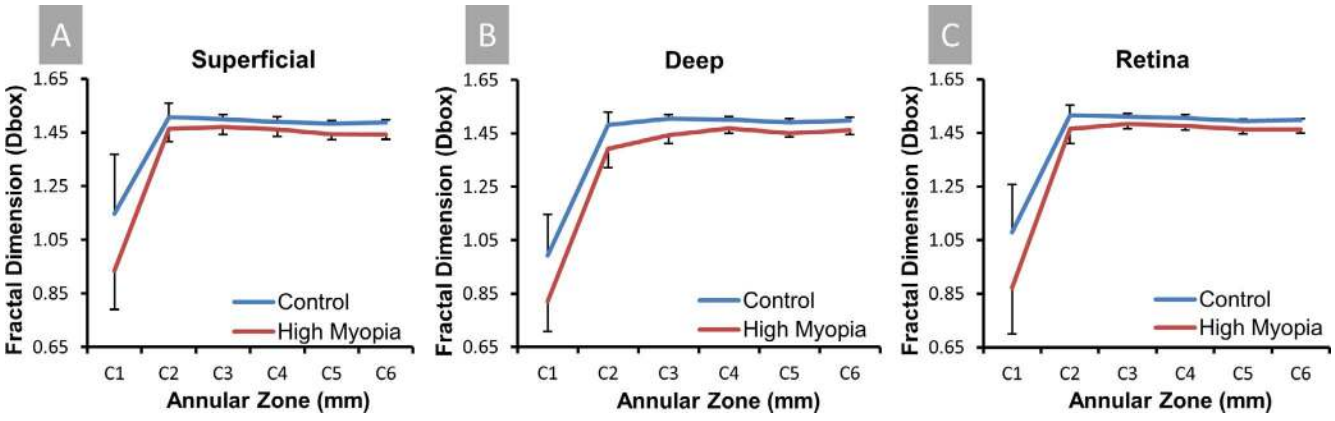

Figure 7. Comparison of the microvessel density (D_{box}) in the six annular zones of the different layers between highly myopic and control eyes. Among the six individual annular zones (C1–C6, bandwidth = 0.16 mm), the microvessel densities in the (**A**) superficial, (**B**) deep, and (**C**) whole retinal layers were all significantly lower in highly myopic eyes than in the control eyes (all $P < 0.05$).

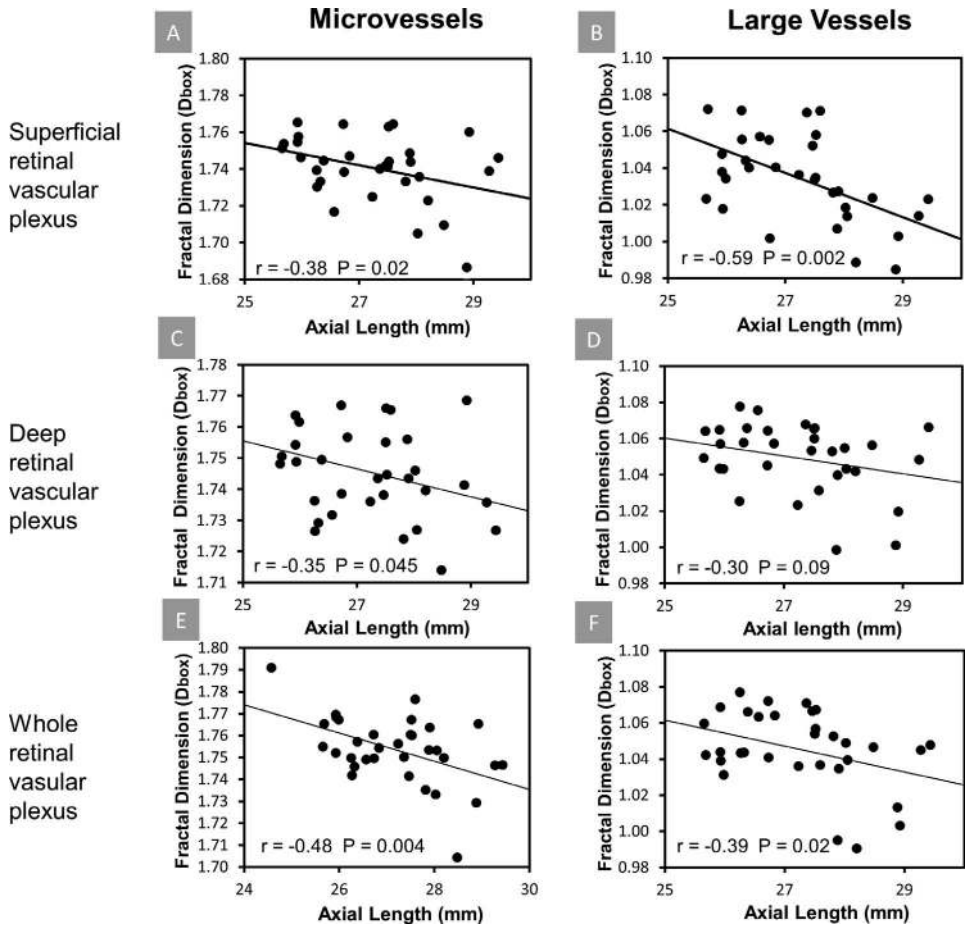

Figure 8. Correlation analyses between retinal vessel density and axial length in each retinal layer. The densities (D_{box}) of microvessels (**A**) and large vessels (**B**) in the superficial and deep (**C**) retinal layers were correlated with axial length elongation. There was no correlation between the density of large vessels and axial length elongation in the deep retinal layer (**D**). The densities of the microvessels (**E**) and large vessels (**F**) were correlated with axial length enlargement in the whole retinal layer.

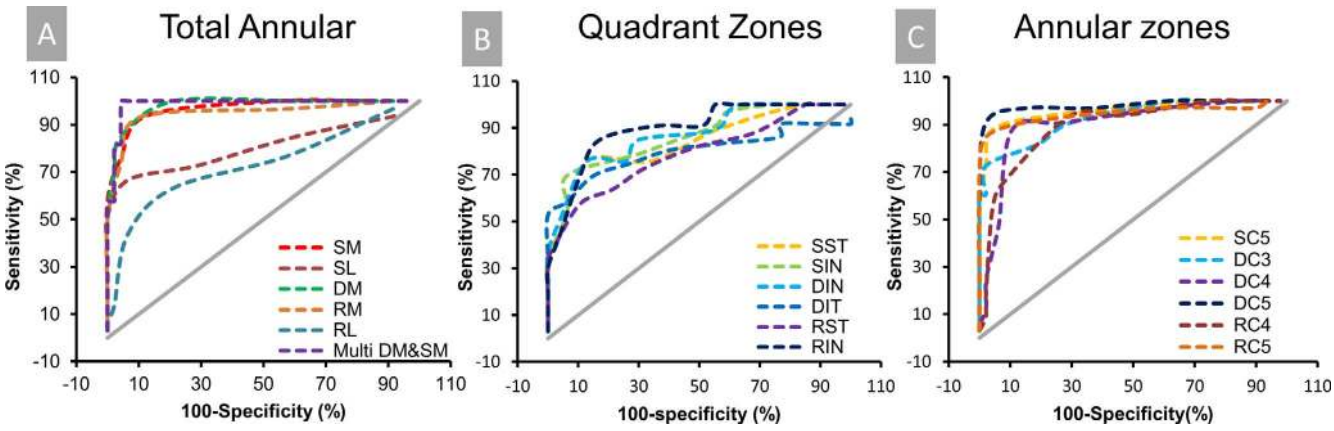

Figure 9. ROC curve analysis of retinal vessels in different annular and quadrantal zones. (**A**) The ROC curves of the microvessel and large vessel densities in the total annular zones for all retinal layers. The combined microvessel density from the superficial and deep retinal layers yielded the highest AUC value (0.987, $P < 0.001$). (**B**) The six largest ROC curve AUC values in the four quadrantal zones of all layers for both microvessels and large vessels. (**C**) The six largest ROC curve AUC values in the six individual annular zones of all layers for both microvessels and large vessels. The AUC values of the C5 microvessel density (1.88–2.2 mm) in the superficial, deep, and whole retinal layers had similar values (0.96, 0.98, and 0.96). SM, superficial microvessels; SL, superficial large vessels; DM, deep retina microvessels; RM, combined retinal microvessels; RL, the whole retina large vessels; SST, superficial superior temporal; SIN, superficial inferior nasal; DIN, deep inferior nasal; RST, retinal superior temporal; RIN, retinal inferior nasal; SC5, superficial C5; DC3, deep C3; DC4, deep C4; DC5, deep C5; RC4, retina C4; RC5, retina C5.

Table 3. Retinal Vasculature Alterations in Myopic Eyes

Authors	Year	Vessel	Instrument	Alteration
Present study	2016	Retinal micro- and large vessels	OCTA	Density decrease
Benavente-Perez et al.[5]	2010	Retrobulbar microvessels	Color Doppler Heidelberg retinal flowmetry	CRA blood velocity decrease. Capillary blood parameters no change
Chueng et al.[22]	2007	Retinal vascular caliber	Retinal photographs	No change
Shimada et al.[24]	2004	Retinal vessels	Laser Doppler velocimetry	CRA blood flow decrease
La Spina et al.[25]	2015	Retina vessels	Dynamic Vessel Analyzer (DVA)	Vessel diameter decrease
Dimitrova et al.[26]	2002	Retrobulbar vessels	Color Doppler imaging	Central retinal vessel velocity decrease
Li et al.[19]	2010	Retina large vessels	Optic disc photographs	Density decrease
Azemin et al.[6]	2014	Retina large vessels	NAVIS Lite Image Filing System	Density decrease
Lim et al.[27]	2011	Retina large vessels	Retinal fundus photographs	Retinal vessel density decrease
Li et al.[20]	2011	Retina large vessels	Fundus camera	Retinal vessel density decrease
Kaneko et al.[28]	2014	Retina large vessels	Fluorescein angiography (FA)	Perfusion area density decrease
Hollo et al.[23]	1997	Peripapillary capillaries	Heidelberg Retina Flowmeter	Capillary perfusion density decrease

CRA, central retinal artery.

not be directly comparable to the changes in vessel density (unit %). Using vessel density analysis, Pinhas et al.[34] documented approximately 20% retinal vessel loss in patients with diabetic retinopathy. In contrast, there was approximately a 1.7% difference in the present study after fractal analysis. Previous studies using fractal analysis of the retinal vessel tree in fundus images demonstrated small changes, which were statistically significant in patients with diabetic retinopathy (0.56%), cognitive dysfunction (0.87%), and stroke (0.3%) compared with controls.[35–37] Our previous study using noninvasive capillary perfusion maps acquired with the Retinal Function Imager (RFI) to study retinal microvascular impairment in patients with multiple sclerosis (MS) found a significant decrease in fractal dimension (0.54%).[38] The decrease (D_{box} 1.7%) in myopic eyes found in the present study was apparently higher than those in previous studies using fractal analyses. The level of vascularity loss may be physiologically significant. Further studies comparing vessel density and fractal dimension in the quantification of retinal vessel density may address the comparability between these two quantitative approaches. The Optovue system currently does not provide a function for correcting the magnification of the highly myopic eyes, so no percentage vessel density values were computed in the present study.

We noticed that the fractal dimension representing vascular density in the whole retina was slightly higher than that in each of the individual layers (Fig. 7). To validate the results, we overlaid superficial and deep vascular layers of five normal eyes and five myopic eyes, and the combined images were processed and compared to the results obtained from the whole retina. The results were almost identical, indicating that the vascular network in the superficial layer covers the majority of the deep vascular network. Therefore, the results for the whole retina appear to reflect mainly the superficial vascular network. Retinal capillary diameter was approximately 5.1 ± 1.4 μm near the avascular zone,[39] and the diameter of isolated human retinal arterioles ranged from 32 to 64 μm.[40] By setting an arbitrary cutoff of 25 μm, the second and third branches of the vessels were successfully separated as evident in Figure 2.

However, some limitations to the present study exist. Although significant retinal vascular density differences between highly myopic and control eyes were successfully demonstrated, the sample size was relatively small for both groups. According to the C_OR of the D_{box} values, we calculated the sample size with G*Power (version 3.1.9).[41] The sample size was 18 for each group when we set the effect size to 1 and the detection power to 90%. In this study, we included 21 subjects in the high myopia group and 24 subjects in the normal control group, which allowed us to test the true differences between groups. Additionally, the relationship between microvascular network alteration and retinal thickness was not calculated. We noticed that the thickness measurements obtained with the commercial system need to be corrected by a magnification step, which is currently not possible for the proprietary software provided with the OCTA instrument. Finally, despite the availability of a larger field of view (6 × 6 mm²), we used the smaller field (3 × 3 mm²) to ensure that image quality would be sufficient for our analyses. Additional work may focus on adapting the method for large-field images. The lateral optical resolution in myopic eyes degrades due to the larger point spread function caused by axial elongation. In myopic eyes, the vessel would appear smaller or thinner, and the vascular network would appear denser in the raw image. The applied magnification correction corrects for differences in the field of view but not lateral optical resolution in myopic eyes, potentially resulting in slightly larger estimates of vessel diameters in these eyes. We used 25 μm as the cutoff to separate the large vessels from both superficial and deep vascular networks. Because of the very small portion of large vessels in the retina compared to the dense microvessel network, the worsening lateral optical coherence resolution may not heavily impact the vessel grouping. To determine if the vessel width threshold was affected by the separation of large vessels, we processed all the images without the large vessels separated, and the results were similar (Table 2). Furthermore, vessel skeletonization may further reduce the potential error, because the method thins the vessel into one pixel line. On the other hand, if the larger appearance of the vessels in myopic eyes induced the shift from the small vessel group to the large vessel group in the superficial layer, we would have found increased large vessels in the retina and superficial vascular network. We actually found significant decreases in the large vessels in both the whole retina and superficial layers. Therefore, the error caused by decreased lateral optical resolution may be insignificant.

Eye movements during imaging may be a more severe problem in highly myopic eyes. To obtain a high-quality retinal vessel network image, automatic focusing with an adaptation for refractive status needs to be used to obtain a sharp internal fixation target for highly myopic eyes. In the present study, we used the built-in image optimization function (Auto All) to obtain the highest-quality image from each study subject. We set the inclusion as a SSI > 40. The eye movement can be offset during image processing with a function known as Motion Correction Technology (MCT) to correct the horizontal and

vertical scans.[11] By visual inspection, we noticed two cases with failed MCT correction, both of which were excluded. One case showed double network images due to excessive motion during image acquisition. The other case showed nine straight lines in the image.

In conclusion, we uncovered and characterized retinal vascular density alterations in highly myopic eyes, which appears to occur in a diffuse manner throughout the retina of highly myopic individuals. The microvascular alterations correlated with AL elongation, and the combined density of the superficial and deep retinal vascular plexus presented the highest discriminating power to assess vascular alteration in high myopia, which may constitute an early indicator of macular retinopathy. Collectively, the use of fractal analyses to quantitatively assess retinal microvasculature changes from OCTA images may help elucidate the underlying pathophysiological mechanisms affecting highly myopic eyes.

Acknowledgments

The authors thank James T. Banta, MD, for proofreading the final manuscript.

Supported by research grants from the National Major Equipment Program of China (2012YQ12008004 to FL) and the National Nature Science Foundation of China (Grant No. 81170869 and Grant No. 81570880 to FL, Grant No. 81400441 to MS).

Disclosure: **Y. Yang**, None; **J. Wang**, None; **H. Jiang**, None; **X. Yang**, None; **L. Feng**, None; **L. Hu**, None; **L. Wang**, None; **F. Lu**, None; **M. Shen**, None

References

1. Pan CW, Zheng YF, Anuar AR, et al. Prevalence of refractive errors in a multiethnic Asian population: the Singapore epidemiology of eye disease study. *Invest Ophthalmol Vis Sci*. 2013;54:2590–2598.
2. Wu LJ, You QS, Duan JL, et al. Prevalence and associated factors of myopia in high-school students in Beijing. *PLoS One*. 2015;10:e0120764.
3. Cho BJ, Shin JY, Yu HG. Complications of pathologic myopia. *Eye Contact Lens*. 2016;42:9–15.
4. Costanzo E, Miere A, Querques G, et al. Type 1 choroidal neovascularization lesion size: indocyanine green angiography versus optical coherence tomography angiography. *Invest Ophthalmol Vis Sci*. 2016;57:OCT307–OCT313.
5. Benavente-Perez A, Hosking SL, Logan NS, Broadway DC. Ocular blood flow measurements in healthy human myopic eyes. *Graefes Arch Clin Exp Ophthalmol*. 2010;248:1587–1594.
6. Azemin MZ, Daud NM, Ab HF, Zahari I, Sapuan AH. Influence of refractive condition on retinal vasculature complexity in younger subjects. *Scientific World Journal*. 2014;2014:783525.
7. Teussink MM, Breukink MB, van Grinsven MJ, et al. OCT angiography compared to fluorescein and indocyanine green angiography in chronic central serous chorioretinopathy. *Invest Ophthalmol Vis Sci*. 2015;56:5229–5237.
8. Toto L, Borrelli E, Di AL, Carpineto P, Mastropasqua R. Retinal vascular plexuses' changes in dry age-related macular degeneration, evaluated by means of optical coherence tomography angiography. *Retina*. 2016;36:1566–1572.
9. Shahlaee A, Samara WA, Hsu J, et al. In vivo assessment of macular vascular density in healthy human eyes using optical coherence tomography angiography. *Am J Ophthalmol*. 2016;165:39–46.
10. Jiang H, Debuc DC, Rundek T, et al. Automated segmentation and fractal analysis of high-resolution non-invasive capillary perfusion maps of the human retina. *Microvasc Res*. 2013;89:172–175.
11. Kraus MF, Potsaid B, Mayer MA, et al. Motion correction in optical coherence tomography volumes on a per A-scan basis using orthogonal scan patterns. *Biomed Opt Express*. 2012;3:1182–1199.
12. Huang D, Jia Y, Gao SS, Lumbroso B, Rispoli M. Optical coherence tomography angiography using the Optovue device. *Dev Ophthalmol*. 2016;56:6–12.
13. Jia Y, Tan O, Tokayer J, et al. Split-spectrum amplitude-decorrelation angiography with optical coherence tomography. *Opt Express*. 2012;20:4710–4725.
14. Ishibazawa A, Nagaoka T, Takahashi A, et al. Optical coherence tomography angiography in diabetic retinopathy: a prospective pilot study. *Am J Ophthalmol*. 2015;160:35–44.
15. Kur J, Newman EA, Chan-Ling T. Cellular and physiological mechanisms underlying blood flow regulation in the retina and choroid in health and disease. *Prog Retin Eye Res*. 2012;31:377–406.
16. Bennett AG, Rudnicka AR, Edgar DF. Improvements on Littmann's method of determining the size of retinal features by fundus photography. *Graefes Arch Clin Exp Ophthalmol*. 1994;232:361–367.
17. Nowroozizadeh S, Cirineo N, Amini N, et al. Influence of correction of ocular magnification on spectral-domain OCT retinal nerve fiber layer measurement variability and performance. *Invest Ophthalmol Vis Sci*. 2014;55:3439–3446.
18. Zhang M, Hwang TS, Campbell JP, et al. Projection-resolved optical coherence tomographic angiography. *Biomed Opt Express*. 2016;7:816–828.
19. Li H, Mitchell P, Liew G, et al. Lens opacity and refractive influences on the measurement of retinal vascular fractal dimension. *Acta Ophthalmol*. 2010;88:e234–e240.
20. Li H, Mitchell P, Rochtchina E, et al. Retinal vessel caliber and myopic retinopathy: the blue mountains eye study. *Ophthalmic Epidemiol*. 2011;18:275–280.
21. Kuehlewein L, Sadda SR, Sarraf D. OCT angiography and sequential quantitative analysis of type 2 neovascularization after ranibizumab therapy. *Eye (Lond)*. 2015;29:932–935.
22. Cheung N, Tikellis G, Saw SM, et al. Relationship of axial length and retinal vascular caliber in children. *Am J Ophthalmol*. 2007;144:658–662.
23. Hollo G, Greve EL, van den Berg TJ, Vargha P. Evaluation of the peripapillary circulation in healthy and glaucoma eyes with scanning laser Doppler flowmetry. *Int Ophthalmol*. 1996;20:71–77.
24. Shimada N, Ohno-Matsui K, Harino S, et al. Reduction of retinal blood flow in high myopia. *Graefes Arch Clin Exp Ophthalmol*. 2004;242:284–288.
25. La Spina C, Corvi F, Bandello F, Querques G. Static characteristics and dynamic functionality of retinal vessels in longer eyes with or without pathologic myopia. *Graefes Arch Clin Exp Ophthalmol*. 2015;254:827–834.
26. Dimitrova G, Tamaki Y, Kato S, Nagahara M. Retrobulbar circulation in myopic patients with or without myopic choroidal neovascularisation. *Br J Ophthalmol*. 2002;86:771–773.
27. Lim LS, Cheung CY, Lin X, et al. Influence of refractive error and axial length on retinal vessel geometric characteristics. *Invest Ophthalmol Vis Sci*. 2011;52:669–678.
28. Kaneko Y, Moriyama M, Hirahara S, Ogura Y, Ohno-Matsui K. Areas of nonperfusion in peripheral retina of eyes with pathologic myopia detected by ultra-widefield fluorescein angiography. *Invest Ophthalmol Vis Sci*. 2014;55:1432–1439.
29. Gadde SG, Anegondi N, Bhanushali D, et al. Quantification of vessel density in retinal optical coherence tomography

Investigative Ophthalmology & Visual Science

angiography images using local fractal dimension. *Invest Ophthalmol Vis Sci*. 2016;57:246–252.

30. Yu J, Jiang C, Wang X, et al. Macular perfusion in healthy Chinese: an optical coherence tomography angiogram study. *Invest Ophthalmol Vis Sci*. 2015;56:3212–3217.
31. Jia Y, Bailey ST, Hwang TS, et al. Quantitative optical coherence tomography angiography of vascular abnormalities in the living human eye. *Proc Natl Acad Sci U S A*. 2015;112:E2395–E2402.
32. Zhao Z, Zhou X, Jiang C, Sun X. Effects of myopia on different areas and layers of the macula: a Fourier-domain optical coherence tomography study of a Chinese cohort. *BMC Ophthalmol*. 2015;15:90.
33. Luu CD, Lau AM, Koh AH, Tan D. Multifocal electroretinogram in children on atropine treatment for myopia. *Br J Ophthalmol*. 2005;89:151–153.
34. Pinhas A, Razeen M, Dubow M, et al. Assessment of perfused foveal microvascular density and identification of nonperfused capillaries in healthy and vasculopathic eyes. *Invest Ophthalmol Vis Sci*. 2014;55:8056–8066.
35. Talu S, Calugaru DM, Lupascu CA. Characterisation of human non-proliferative diabetic retinopathy using the fractal analysis. *Int J Ophthalmol*. 2015;8:770–776.
36. Aliahmad B, Kumar DK, Hao H, et al. Zone specific fractal dimension of retinal images as predictor of stroke incidence. *Scientific World Journal*. 2014;2014:467462.
37. Cheung CY, Ong S, Ikram MK, et al. Retinal vascular fractal dimension is associated with cognitive dysfunction. *J Stroke Cerebrovasc Dis*. 2014;23:43–50.
38. Jiang H, Delgado S, Liu C, et al. In vivo characterization of retinal microvascular network in multiple sclerosis. *Ophthalmology*. 2016;123:437–438.
39. Wang Q, Kocaoglu OP, Cense B, et al. Imaging retinal capillaries using ultrahigh-resolution optical coherence tomography and adaptive optics. *Invest Ophthalmol Vis Sci*. 2011;52:6292–6299.
40. Hein TW, Rosa RH Jr, Yuan Z, Roberts E, Kuo L. Divergent roles of nitric oxide and rho kinase in vasomotor regulation of human retinal arterioles. *Invest Ophthalmol Vis Sci*. 2010;51:1583–1590.
41. Faul F, Erdfelder E, Lang AG, Buchner A. G*Power 3: a flexible statistical power analysis program for the social, behavioral, and biomedical sciences. *Behav Res Methods*. 2007;39:175–191.

Investigative Ophthalmology & Visual Science